

Bit-Metric Decoding Rate in Multi-User MIMO Systems: Theory

K. Pavan Srinath and Jakob Hoydis, *Senior Member, IEEE*

Abstract

Link-adaptation (LA) is one of the most important aspects of wireless communications where the modulation and coding scheme (MCS) used by the transmitter is adapted to the channel conditions in order to meet a certain target error-rate. In a single-user SISO (SU-SISO) system, LA is performed by computing the post-equalization signal-to-interference-noise ratio (SINR) at the receiver. The same technique can be employed in multi-user MIMO (MU-MIMO) receivers that use linear detectors. Another important use of post-equalization SINR is for physical layer (PHY) abstraction, where several PHY blocks like the channel encoder, the detector, and the channel decoder are replaced by an abstraction model in order to speed up system-level simulations. This is achieved by mapping the post-equalization SINR to a codeword error rate (CER) or a block error rate (BLER). However, for MU-MIMO systems with non-linear receivers, like those that use variants of the sphere-decoder algorithm, there is no known equivalent of post-equalization SINR which makes both LA and PHY abstraction extremely challenging. This important issue is addressed in this two-part paper. A metric called the bit-metric decoding rate (BMDR) of a detector for a set of channel realizations is presented in this part. BMDR is the proposed equivalent of post-equalization SINR for arbitrary detectors. Since BMDR does not have a closed form expression that would enable its instantaneous calculation, a machine-learning approach to predict it is presented. The second part describes the algorithms to perform LA, detector selection, and PHY abstraction using BMDR for MU-MIMO systems with arbitrary detectors. Extensive simulation results corroborating the claims are presented.

Index Terms

Bit-metric decoding rate (BMDR), convolutional neural network (CNN), linear minimum mean square error (LMMSE), link-adaptation (LA), K -best detector, multi-user MIMO (MU-MIMO), orthogonal frequency division multiplexing (OFDM), physical layer (PHY) abstraction.

K. P. Srinath is with Nokia Bell Labs, 91620 Nozay, France (email: pavan.koteshwar_srinath@nokia-bell-labs.com), and J. Hoydis is with NVIDIA, 06906 Sophia Antipolis, France (email: jhoydis@nvidia.com). A significant part of this work was done when J. Hoydis was at Nokia Bell Labs, 91620 Nozay, France.

I. INTRODUCTION

Next-generation wireless technologies such as 5G New Radio (5G NR) are designed to deliver high levels of performance and efficiency that enable a wide range of 5G services like enhanced mobile broadband (eMBB) and ultra-reliable low-latency communications (uRLLC). Advanced multiple-input multiple-output (MIMO) transmission techniques, wideband orthogonal frequency division multiplexing (OFDM), and strong channel coding schemes are some important features of these technologies. One of the most difficult challenges in a MIMO system is the joint detection of the signal components. The task of a MIMO detector is to generate soft-information, usually in the form of log-likelihood ratio (LLR), for each transmitted bit of each user. This soft-information is used by the channel decoder to recover the transmitted message bits. There exist many MIMO detection techniques in the literature, ranging from simple linear detectors like the linear minimum mean square error (LMMSE) detector [1, Ch. 8], [2] to the more computationally-expensive maximum-likelihood (ML)-based sphere-decoder [3], [4]. There are several detectors whose computational complexity and reliability lie in between that of the LMMSE detector and the sphere-decoder, a couple of them being the fixed-complexity sphere-decoder [5] and the K -best detector [6]. Other non-linear detectors that are not based on sphere-decoding include iterative soft interference cancellation (SIC) [7] and machine-learning-based receivers (see [8], and references therein). While the LMMSE detector is quite popular due to its low complexity, non-linear detectors will likely play an increasingly important role for next-generation MIMO systems.

A. Motivation

The following two important use cases in advanced wireless communication systems serve as motivation for this work.

1) *Link-adaptation (LA)*: One of the most important aspects of high-rate and reliable wireless communication systems is LA. This feature enables a transmitter to adapt its modulation and coding scheme (MCS) to the current channel conditions in order to meet a certain target codeword error rate (CER) or block error rate (BLER), where a block can consist of several codewords [9, Section 5]. This allows the transmitter and the receiver to reliably communicate at near-optimal data-rates that the channel supports. In single-input single-output (SISO) systems, post-equalization signal-to-interference-noise ratio (SINR) is a sufficient metric to identify the most suitable MCS [10]–[12]. This also holds true for multi-user MIMO (MU-MIMO) systems

with linear receivers; for example, those receivers that use the LMMSE detector. This is because linear receivers allow the computation of post-equalization SINR for each user, which, when accurate enough, can be mapped to the best available MCS. However, for MU-MIMO systems with non-linear receivers, a metric equivalent to post-equalization SINR is not currently known in the literature. This makes LA very challenging in such systems.

2) *Physical layer (PHY) abstraction*: Base station (BS) and user-equipment (UE) manufacturers use system-level simulations (SLS) to evaluate the performance of their algorithms. A typical system-level simulator is composed of (but not limited to) the following functionalities: intercell-interference modelling, resource scheduling and resource allocation, power allocation and power control, link-adaptation block with channel quality feedback, channel modeling, and link performance modeling. The link-performance-modeling block models the PHY components of the communication system. Some components of this block (channel encoding, detection, channel decoding, etc.) are time-intensive and computation-intensive to simulate. So, in order to reduce the complexity of SLS, these components are replaced by simpler functionalities that are quick to execute but capture the essential behavior of the overall physical layer. This technique is called PHY abstraction. The precise goal of PHY abstraction is to obtain the same figures of merit for performance evaluation as would be obtained if the original components were used, but with much simpler complexity. In the literature, there exist abstraction models for SISO systems ([13], and references therein), and (with some limitations) for MU-MIMO systems with linear receivers. These work by mapping post-equalization SINR to CER/BLER. However, there is no known technique to perform PHY abstraction for non-linear MU-MIMO receivers since there is no known metric equivalent to post-equalization SINR for such receivers.

In this two-part paper, we address the aforementioned issues. The contributions of this part of the two-part paper may be summarized as follows:

- We introduce the notion of bit-metric decoding rate (BMDR) of a MIMO detector for a given channel realization or a set of channel realizations. BMDR is our proposed equivalent of post-equalization SINR for arbitrary receivers. We establish the relationship between BMDR, the channel code-rate, and the CER (see Theorem 1 in Section III).
- We present a machine-learning-based method to estimate the BMDR of a detector for a set of observed channel realizations. The need for a machine-learning-based approach is due to the fact that BMDR does not have a closed-form expression or any other straightforward method of calculating it in real time.

- We provide extensive simulations results to highlight the efficacy of our proposed method.

In the second part [14], the results obtained here are utilized to describe new techniques to perform LA and PHY abstraction in MU-MIMO systems with arbitrary receivers.

B. Related Literature

There have been a few metrics in the literature that are used in lieu of SINR. Some important ones are mutual-information (MI) [15], capacity of coded-modulation [16], and capacity of bit-interleaved coded modulation (BICM) [16]. However, these are general information-theoretic metrics for a chosen input constellation, and do not take into consideration the effect of a given specific receiver. Very few papers [17], [18] have proposed information-theoretic metrics that are relevant to a given MIMO detector. However, the metric considered in these papers requires the distribution of LLRs which is not straightforward to compute in real time, and the approximation in [18] holds for a specific 2×2 MIMO system with an ML receiver. To the best of our knowledge, there is no work in the literature that presents a metric equivalent to post-equalization SINR for arbitrary receivers with a practical method to compute it in real time.

Paper Organization

The system model and a few relevant definitions are presented in Section II. Section III introduces the BMDR and analyses its relevance to error performance. Section IV describes the challenges in predicting BMDR while Section V details how machine-learning can be employed to perform BMDR-prediction. Simulation results showing the efficacy of the proposed BMDR-prediction method for K -best detector are presented in Section VI, and the concluding remarks are made in Section VII.

Notation

Boldface upper-case (lower-case) letters denote random matrices (vectors), and normal upright upper-case (lower-case) letters are understood from context to denote the realizations of random matrices (vectors). Similarly, if \mathcal{B} denotes a set of random variables, then \mathcal{B} denotes the set of the realizations of the individual random variables. The field of complex numbers, the field of real numbers, and the ring of integers are respectively denoted by \mathbb{C} , \mathbb{R} , and \mathbb{Z} . For any set \mathcal{S} , $|\mathcal{S}|$ denotes its cardinality if it is finite, and the subset of positive elements in \mathcal{S} is denoted by \mathcal{S}_+ . The notation $\mathbf{X} \in \mathcal{S}^{m \times n}$ denotes that \mathbf{X} is a matrix of size $m \times n$ with each entry taking values

from a set \mathcal{S} . For a matrix \mathbf{X} , its transpose and Hermitian transpose are respectively denoted by \mathbf{X}^T and \mathbf{X}^H , Frobenius norm by $\|\mathbf{X}\|$, and its $(i, j)^{th}$ entry by $[\mathbf{X}]_{i,j}$ or $\mathbf{X}_{i,j}$ depending on convenience. The block-diagonal matrix with diagonal blocks $\mathbf{D}_1, \mathbf{D}_2, \dots, \mathbf{D}_n$ is denoted by $\text{diag}(\mathbf{D}_1, \mathbf{D}_2, \dots, \mathbf{D}_n)$, and the same notation is used for denoting a diagonal matrix with diagonal elements d_1, \dots, d_n . The identity matrix of size $n \times n$ is denoted by \mathbf{I}_n . The notation $\mathbf{n} \sim \mathcal{CN}(0, \mathbf{I}_n)$, $\mathbf{n} \sim \mathcal{N}(0, \mathbf{I}_n)$, and $\mathbf{n} \sim \mathcal{U}(\mathcal{S})$ respectively denote that \mathbf{n} is sampled from the n -dimensional complex standard normal distribution, the standard normal distribution, and the uniform distribution from a set \mathcal{S} . For a matrix $\mathbf{X} \in \mathbb{C}^{m \times n}$ and a vector $\mathbf{x} \in \mathbb{C}^{n \times 1}$,

$$\mathbf{X}^{\mathcal{R}} \triangleq \begin{bmatrix} \Re(\mathbf{X}) & -\Im(\mathbf{X}) \\ \Im(\mathbf{X}) & \Re(\mathbf{X}) \end{bmatrix} \in \mathbb{R}^{2m \times 2n}, \quad \mathbf{x}^{\mathcal{R}} \triangleq \begin{bmatrix} \Re(\mathbf{x}) \\ \Im(\mathbf{x}) \end{bmatrix} \in \mathbb{R}^{2n \times 1}, \quad (1)$$

where $\Re(\mathbf{X}) \in \mathbb{R}^{m \times n}$ and $\Im(\mathbf{X}) \in \mathbb{R}^{m \times n}$ denote the entry-wise real and imaginary parts of \mathbf{X} , respectively. The map of an element x in the set \mathcal{X} according to a predefined one-to-one mapping rule is denoted by $\text{MAP}\{x; \mathcal{X}\}$, and x can be a tuple. Finally, $\text{Sample}(D)$ denotes a sample drawn from the distribution D . The natural logarithm is denoted by $\ln()$.

II. SYSTEM MODEL AND DEFINITIONS

We consider an OFDM-based MIMO communication system in this paper, but the following technical content is applicable to any communication system in general. Suppose that there are $n_r \geq 1$ receive antennas and $N_u \geq 1$ UEs, with UE i being equipped with $n_t^{(i)}$ transmit antennas, $i = 1, \dots, N_u$. Let $\sum_{i=1}^{N_u} n_t^{(i)} = N \leq n_r$. A block diagram of the uplink transmission in such a system is depicted in Fig. 1. This setup could also be applied for the downlink.

We consider the classic BICM [16] for MU-MIMO systems. For UE i , the message set $\mathcal{W}_i = \{w_j, j = 1, \dots, 2^{k_i}\}$ consists of 2^{k_i} messages for some positive integer k_i . The channel encoder \mathcal{E}_i , given as,

$$\begin{aligned} \mathcal{E}_i : \mathcal{W}_i &\longrightarrow \mathcal{C}_i \subset \{0, 1\}^{n_i}, \\ w &\longmapsto \mathcal{E}_i(w) \in \mathcal{C}_i, \end{aligned}$$

maps each message to an n_i -bit codeword, thereby yielding a code-rate of $k_i/n_i \leq 1$. The codeword bits are then interleaved across the entire codeword using an interleaver denoted by π_i . The interleaver essentially permutes the order of the codeword bit sequence, and hence, is invertible at the receiver.

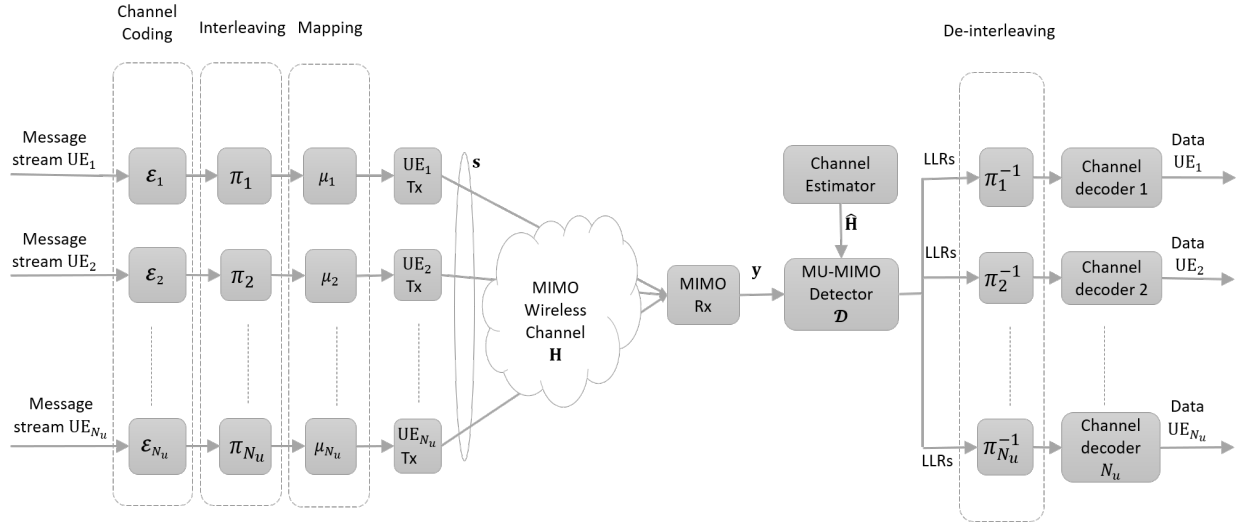


Fig. 1: Uplink transmission in a general multi-user MIMO system.

The OFDM system uses N_{sc} subcarriers, and a resource element (RE) consists of one subcarrier and one time symbol. Throughout the rest of the paper, we use the pair (f, t) to index an RE, with f denoting the subcarrier index and t denoting the symbol. We assume that UE i uses a unit-energy complex constellation for modulation, denoted by \mathcal{Q}_i . The size of \mathcal{Q}_i is 2^{m_i} for some $m_i \in 2\mathbb{Z}_+$. We do not consider transmit-precoding in this paper and assume that the number of spatial streams transmitted by each UE is equal to the number of its transmit antennas. However, a generalization to the case where there is transmit-precoding and the number of spatial streams is lower is straightforward by integrating the precoder in the channel matrix. So, every RE is associated with $m_i n_t^{(i)}$ bits of UE i , and the n_i interleaved codeword bits are transmitted over $n_i / (m_i n_t^{(i)})$ REs (assuming $m_i n_t^{(i)}$ divides n_i). Let the interleaved bits of the codeword $\mathcal{E}_i(w)$ that are transmitted on the RE indexed by the pair (f, t) be denoted by $b_{f,t,i,l,j}(w)$, $l = 1, \dots, n_t^{(i)}$, $j = 1, \dots, m_i$. We denote the set of these bits by $\mathcal{B}_{f,t,i}(w) = \{b_{f,t,i,l,j}(w), l = 1, \dots, n_t^{(i)}, j = 1, \dots, m_i\}$, and we denote by $\mathcal{B}_{f,t,i} \triangleq \{b_{f,t,i,l,j}, l = 1, \dots, n_t^{(i)}, j = 1, \dots, m_i\}$ the random set of bits whose realizations are $\mathcal{B}_{f,t,i}(w)$, $w \in \mathcal{W}_i$. It is quite common for current generation communication systems to use a *scrambler* [19, 5.3.1] on the codeword bits. Next, a mapper μ_i , which is a bijective map defined as

$$\mu_i : \{0, 1\}^{n_t^{(i)} \times m_i} \longrightarrow \mathcal{Q}_i^{n_t^{(i)} \times 1},$$

$$\mathcal{B}_{f,t,i}(w) \longmapsto \mathbf{s}_{f,t,i} \in \mathcal{Q}_i^{n_t^{(i)} \times 1},$$

is used to map $\mathcal{B}_{f,t,i}(w)$ (or their scrambled bits) to a constellation symbol vector $\mathbf{s}_{f,t,i} \in \mathcal{Q}_i^{n_t^{(i)} \times 1}$ by mapping groups of m_i bits to a point in \mathcal{Q}_i . The UE then uses a total transmit power ρ_i to transmit this symbol vector over the channel with channel matrix $\mathbf{H}_{f,t,i} \in \mathbb{C}^{n_r \times n_t^{(i)}}$. As mentioned earlier, when UE i uses a transmit-precoder $\mathbf{W}_i \in \mathbb{C}^{n_t^{(i)} \times n_t^{(i)}}$ to transmit $n_l^{(i)} \leq n_t^{(i)}$ spatial streams, its effective channel matrix is $\mathbf{H}_{f,t,i}\mathbf{W}_i$. Let \mathcal{G}_i denote the set of RE index pairs over which the codeword for UE i is transmitted. After cyclic-prefix removal and discrete Fourier transform at the receiver, the complex-baseband signal model for an RE indexed by (f, t) is given as

$$\mathbf{y}_{f,t} = \sum_{i=1}^{N_u} \sqrt{\frac{\rho_i}{n_t^{(i)}}} \mathbf{H}_{f,t,i} \mathbf{s}_{f,t,i} + \mathbf{n}_{f,t} = \mathbf{H}_{f,t} \mathbf{s}_{f,t} + \mathbf{n}_{f,t} \quad (2)$$

where $\mathbf{H}_{f,t} \triangleq \left[\sqrt{\rho_1/n_t^{(1)}} \mathbf{H}_{f,t,1}, \dots, \sqrt{\rho_{N_u}/n_t^{(N_u)}} \mathbf{H}_{f,t,N_u} \right] \in \mathbb{C}^{n_r \times N}$, $\mathbf{s}_{f,t} \triangleq [\mathbf{s}_{f,t,1}^T, \dots, \mathbf{s}_{f,t,N_u}^T]^T \in \mathcal{Q}^{N \times 1}$ with $\mathcal{Q}^{N \times 1} \triangleq \mathcal{Q}_1^{n_t^{(1)} \times 1} \times \dots \times \mathcal{Q}_{N_u}^{n_t^{(N_u)} \times 1}$, and $\mathbf{n}_{f,t} \sim \mathcal{CN}(0, \mathbf{I}_{n_r})$ represents the complex additive white Gaussian noise (AWGN). It is assumed that the realization of the channel matrix $\mathbf{H}_{f,t}$, denoted by $\mathbf{H}_{f,t}$, for each RE is known perfectly at the receiver, although in practice only an imperfect estimate $\hat{\mathbf{H}}_{f,t}$ is available. Let $\mathcal{Y}_{\mathcal{G}_i} = \{\mathbf{y}_{f,t}, \forall (f, t) \in \mathcal{G}_i\}$ and $\mathcal{H}_{\mathcal{G}_i} \triangleq \{\mathbf{H}_{f,t}, \forall (f, t) \in \mathcal{G}_i\}$ respectively be the set of all received signal vectors and the set of channel matrices corresponding to the transmission of the entire codeword for UE i . We emphasize that $\mathcal{Y}_{\mathcal{G}_i}$ and $\mathcal{H}_{\mathcal{G}_i}$ are random vectors and matrices whose realizations are respectively denoted by $\mathcal{Y}_{\mathcal{G}_i} \triangleq \{\mathbf{y}_{f,t}, (f, t) \in \mathcal{G}_i\}$ and $\mathcal{H}_{\mathcal{G}_i} \triangleq \{\mathbf{H}_{f,t}, (f, t) \in \mathcal{G}_i\}$.

Definition II.1. (Multi-user MIMO Detector) For the MU-MIMO system as described and for the set of constellations $\{\mathcal{Q}_i\}_{i=1}^{N_u}$, a detector \mathcal{D} which is parameterized by n_r , $\{n_t^{(i)}\}_{i=1}^{N_u}$, is a set of N_u maps $\mathcal{D}^{(i)}$, $i = 1, \dots, N_u$, defined as follows.

$$\begin{aligned} \mathcal{D}^{(i)} : \mathbb{C}^{n_r \times 1} \times \mathbb{C}^{n_r \times N} \times \mathcal{Q}^{N \times 1} &\longrightarrow \mathbb{R}^{n_t^{(i)} \times m_i}, \\ (\mathbf{y}_{f,t}, \mathbf{H}_{f,t}; \mathcal{Q}^{N \times 1}) &\longmapsto \mathcal{D}^{(i)}(\mathbf{y}_{f,t}, \mathbf{H}_{f,t}; \mathcal{Q}^{N \times 1}) \in \mathbb{R}^{n_t^{(i)} \times m_i}. \end{aligned}$$

Henceforth, we won't explicitly state $\mathcal{Q}^{N \times 1}$, and the constellation set is assumed from context. Here, $[\mathcal{D}^{(i)}(\mathbf{y}_{f,t}, \mathbf{H}_{f,t})]_{l,j}$ is the LLR for the j^{th} bit on the l^{th} transmit antenna for UE i for the RE in context, and is defined as

$$[\mathcal{D}^{(i)}(\mathbf{y}_{f,t}, \mathbf{H}_{f,t})]_{l,j} = \ln \left(\frac{\mathbb{P}\{b_{f,t,i,l,j} = 1 | \mathbf{y}_{f,t} = \mathbf{y}_{f,t}, \mathbf{H}_{f,t} = \mathbf{H}_{f,t}, \mathcal{D}\}}{\mathbb{P}\{b_{f,t,i,l,j} = 0 | \mathbf{y}_{f,t} = \mathbf{y}_{f,t}, \mathbf{H}_{f,t} = \mathbf{H}_{f,t}, \mathcal{D}\}} \right). \quad (3)$$

Finally, the LLRs for all the codeword bits, after de-interleaving and de-scrambling, are used as inputs to the channel decoder which reconstructs the transmitted message stream. This procedure is called *bit-metric decoding* [20] since the LLRs are metrics associated with each transmitted bit and are used for decoding.

Let $q_{\mathcal{D}}(b_{f,t,i,l,j}; \mathbf{y}_{f,t}, \mathbf{H}_{f,t})$ denote $\mathbb{P}\{b_{f,t,i,l,j} | \mathbf{y}_{f,t} = \mathbf{y}_{f,t}, \mathbf{H}_{f,t} = \mathbf{H}_{f,t}, \mathcal{D}\}$. We have

$$q_{\mathcal{D}}(1; \mathbf{y}_{f,t}, \mathbf{H}_{f,t}) = \frac{1}{1 + \exp\left[-[\mathcal{D}^{(i)}(\mathbf{y}_{f,t}, \mathbf{H}_{f,t})]_{l,j}\right]} = 1 - q_{\mathcal{D}}(0; \mathbf{y}_{f,t}, \mathbf{H}_{f,t}).$$

All practical detectors have an upper bound on the magnitudes of the LLRs that they generate, simply due to the fixed number of bits allocated for LLR values. We denote this bound by L_{max} so that $\forall i \in \{1, \dots, N_u\}$,

$$\mathcal{D}^{(i)} : \mathbb{C}^{n_r \times 1} \times \mathbb{C}^{n_r \times N} \times \mathcal{Q}^{N \times 1} \longrightarrow [-L_{max}, L_{max}]^{n_t^{(i)} \times m_i}. \quad (4)$$

So, we have the following inequality which we use later in the proof of Theorem 1: $\forall b \in \{0, 1\}, \mathbf{y} \in \mathbb{C}^{n_r \times 1}, \mathbf{H} \in \mathbb{C}^{n_r \times N_u}$,

$$-(\log_2(e)L_{max} + 1) < \log_2(q_{\mathcal{D}}(b; \mathbf{y}, \mathbf{H})) < 0. \quad (5)$$

III. BIT-METRIC DECODING RATE

In this section, we introduce the notion of BMDR of a detector for a user's set of channels. Before we proceed, we make the following assumptions which are quite practical. The usage of a sufficiently long channel code with strong error-correcting capabilities in conjunction with a good interleaver and a scrambler will result in an approximately discrete uniform distribution for the bits transmitted on a resource element. To be precise, $\mathbb{P}\{\mathbf{B}_{f,t,i}\} \approx 2^{-m_i n_t^{(i)}}, \forall i = 1, \dots, N_u, \forall (f, t) \in \mathcal{G}_i$. This further implies that $\mathbf{s}_{f,t}$ in (2) also has the discrete uniform distribution, with each user's symbol vector being independent of other users' symbol vectors. With these assumptions, the BMDR of a detector \mathcal{D} for UE i , which is denoted by $R_{\mathcal{D},i}(\mathcal{H})$, for a set of channels \mathcal{H} (this set can be a singleton with just a single channel matrix) is defined as follows.

$$\begin{aligned} R_{\mathcal{D},i}(\mathcal{H}) &\triangleq 1 + \frac{1}{|\mathcal{H}|} \sum_{\mathbf{H}_{f,t} \in \mathcal{H}} \mathbb{E}_{\mathbf{y}_{f,t} | \mathbf{H}_{f,t}} \left[\frac{1}{m_i n_t^{(i)}} \sum_{l=1}^{n_t^{(i)}} \sum_{j=1}^{m_i} \log_2 (q_{\mathcal{D}}(b_{f,t,i,l,j}; \mathbf{y}_{f,t}, \mathbf{H}_{f,t})) \middle| \mathbf{H}_{f,t} \right] \quad (6) \\ &= \frac{1}{|\mathcal{H}|} \sum_{\mathbf{H}_{f,t} \in \mathcal{H}} R_{\mathcal{D},i}(\mathbf{H}_{f,t}) \end{aligned}$$

where $\{b_{f,t,i,l,j}\}_{l,j}$ is related to the elements of $\mathbf{s}_{f,t,i}$ through the bijective map μ_i , and $\mathbf{y}_{f,t}$ is dependent only on $\mathbf{s}_{f,t}$ and $\mathbf{n}_{f,t}$ when conditioned on $\mathbf{H}_{f,t}$. Note that $R_{\mathcal{D},i}(\mathcal{H})$ is itself a random variable whose realization is dependent on the realizations of the channel matrices $\mathbf{H}_{f,t}$.

We are interested in the codeword error behavior for a set of channel realizations $\mathcal{H}_{\mathcal{G}_i}$ over which the codeword is transmitted when \mathcal{D} is used.

Theorem 1. *Consider a sequence of sets of channel realizations $\{\mathcal{H}_{\mathcal{G}_i(n)} \mid |\mathcal{G}_i(n)| = n\}_{n \in \mathbb{Z}_+}$, such that $\inf_{n \in \mathbb{Z}_+} R_{\mathcal{D},i}(\mathcal{H}_{\mathcal{G}_i(n)}) = R_{\mathcal{D},i}^{\min} > 0$. Then, for any $\epsilon \in (0, 1]$, there exists an (n_i, k_i) code $\mathcal{C}_i(n_i)$ with rate $R_{\mathcal{C}_i}(n_i) = \frac{k_i}{n_i}$ and $\delta \in (0, R_{\mathcal{D},i}^{\min})$ such that the probability of codeword error is less than ϵ if $R_{\mathcal{C}_i}(n_i) < R_{\mathcal{D},i}^{\min} - \delta$. Further, any (n_i, k_i) code $\mathcal{C}_i(n_i)$ such that the probability of codeword error is less than ϵ must have $R_{\mathcal{C}_i}(n_i) = \frac{k_i}{n_i} < R_{\mathcal{D},i}^{\min}$.*

The proof is provided in the Appendix. It is shown in the proof that $R_{\mathcal{D},i}(\mathcal{H}_{\mathcal{G}_i})$ represents the normalized MI between the transmitted codeword bits and the detector outputs for a fixed and known set of channel realizations $\mathcal{H}_{\mathcal{G}_i}$. For the case of a maximum-likelihood detector, BMDR is the normalized BICM capacity with perfect channel state information (CSI) for a fixed set of channel realizations. The differentiating feature between BMDR and other metrics in the literature is that BMDR takes into account the effect of a suboptimal detector while most of the known works in the literature do not. We wish to specify here that this theorem holds only for the system model under consideration where the transmitted bits are independent and identically distributed (i.i.d.) (due to the usage of interleaving and scrambling). Further, the proof of Theorem 1 reveals that the probability of codeword error has a strong inverse relationship with the codeword length n_i and the margin $\delta = R_{\mathcal{D},i}(\mathcal{H}_{\mathcal{G}_i}) - k_i/n_i$, and a weak direct relationship with the modulation order m_i .

Here, $R_{\mathcal{D},i}(\mathcal{H}_{\mathcal{G}_i})$ can be interpreted as follows: If the set of channel realizations $\mathcal{H}_{\mathcal{G}_i}$ were fixed for several codeword transmissions and a detector \mathcal{D} is used, then, UE i could transmit reliably using a code-rate up to $R_{\mathcal{D},i}(\mathcal{H}_{\mathcal{G}_i})$. To illustrate this, we consider a simulation setup using the QuaDRiGa channel-simulator [21]. A (1800, 1200) 5G low-density parity-check (LDPC) code is employed along with QPSK modulation (4-QAM). The base station is set up to have 16 antennas, and there are four users placed at random within a distance of 25–250 m from the base station. The exact details of the channel-generator scenario are presented in Section VI. A sequence of 900 MU-MIMO channel matrices is generated according to the urban macro-cell (UMa) scenario with non-line-of-sight (NLoS) propagation. Let $\{\mathbf{h}_k^{(i)} \in \mathbb{C}^{16 \times 1}, k = 1, \dots, 900\}$

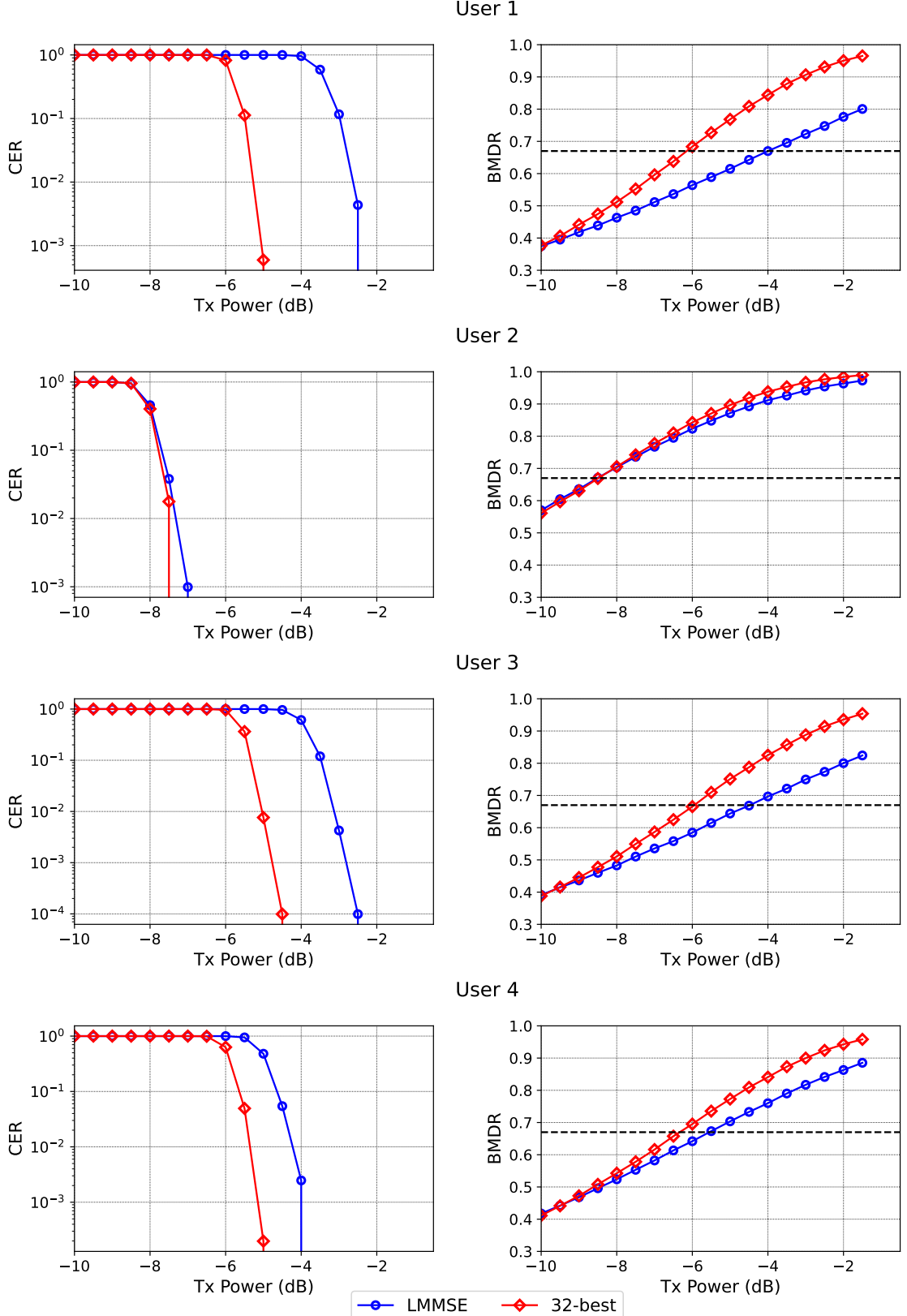


Fig. 2: The CER (left) and BMDR (right) comparison for a fixed set of channel realizations.

denote the channel vectors from UE i to the base station, $i = 1, 2, 3, 4$. This set of 900 channel matrices corresponds to a codeword transmission for each UE. We also have

$$\frac{1}{900} \sum_{k=1}^{900} \left\| \mathbf{h}_k^{(i)} \right\|^2 = 16, \quad i = 1, 2, 3, 4. \quad (7)$$

The CER as a function of the transmit power is plotted in Fig. 2 for the four users with the LMMSE detector and the 32-best detector employed ($K = 32$ for the K -best detector [6]). This is of course not representative of a realistic wireless fading environment where the channel matrices are different for different codeword transmissions, but considered here only to support the claims of Theorem 1. Also plotted to the right of each CER plot is the BMDR (empirically approximated using the methodology outlined in Section IV, to be precise, using (10)) for the two detectors as a function of the same transmit power, and for each user. It can clearly be seen that for all the CER curves, the fall begins after a transmit power corresponding to a BMDR of 0.67 (indicated by the horizontal dashed line in the BMDR plots) has been reached.

A. Imperfect Channel Estimates and Colored Noise

Let $\hat{\mathbf{H}}_{f,t}$ denote the estimated channel so that $\mathbf{H}_{f,t} = \hat{\mathbf{H}}_{f,t} + \Delta\mathbf{H}_{f,t}$ where $\Delta\mathbf{H}_{f,t}$ denotes the estimation error. The signal model of (2) in the presence of interference noise can be written as

$$\mathbf{y}_{f,t} = \hat{\mathbf{H}}_{f,t} \mathbf{s}_{f,t} + \Delta\mathbf{H}_{f,t} \mathbf{s}_{f,t} + \mathbf{n}_{f,t} \quad (8)$$

where the interference noise is subsumed in $\mathbf{n}_{f,t}$ so that $\mathbf{n}_{f,t} \sim \mathcal{CN}(0, \mathbf{K}_n)$, $\mathbf{K}_n \in \mathbb{C}^{n_r \times n_r}$ being a Hermitian, positive-definite but non-diagonal matrix. If an LMMSE estimator is used for channel estimation, then from the orthogonality principle, $\Delta\mathbf{H}_{f,t}$ is uncorrelated with $\mathbf{H}_{f,t}$ [22]. Further, if one has an estimate of the mean and the correlation matrix of $\mathbf{H}_{f,t}$, it is straightforward to estimate the error correlation matrix $\mathbf{K}_e \triangleq \mathbb{E}\{\Delta\mathbf{H}_{f,t} \Delta\mathbf{H}_{f,t}^H\} \in \mathbb{C}^{n_r \times n_r}$. This can also be based on the instantaneous channel statistics if we assume that $\mathbf{H}_{f,t}$ has a non-stationary distribution (see, for example, [23] and references therein). Assuming that $\mathbf{H}_{f,t}$ has zero mean, $\Delta\mathbf{H}_{f,t} \mathbf{s}_{f,t}$ can be approximated by a zero-mean Gaussian noise vector with covariance \mathbf{K}_e since the constellations \mathcal{Q}_i are all assumed to be of unit energy. Noting that $\mathbf{K}_n + \mathbf{K}_e$ is positive-definite and Hermitian, its eigendecomposition yields $\mathbf{K}_n + \mathbf{K}_e = \mathbf{U} \Lambda \mathbf{U}^H$ with Λ being a diagonal matrix with positive

elements. Let $\Lambda^{1/2}$ denote the diagonal matrix with its diagonal entries being the square roots of those of Λ . Therefore, after noise-whitening, the signal model can be expressed as

$$\mathbf{y}'_{f,t} = \mathbf{H}'_{f,t} \mathbf{s}_{f,t} + \mathbf{n}'_{f,t}, \quad (9)$$

where $\mathbf{y}'_{f,t} = (\mathbf{K}_n + \mathbf{K}_e)^{-\frac{1}{2}} \mathbf{y}_{f,t}$, $\mathbf{H}'_{f,t} = (\mathbf{K}_n + \mathbf{K}_e)^{-\frac{1}{2}} \hat{\mathbf{H}}_{f,t}$, and $\mathbf{n}'_{f,t} \sim \mathcal{CN}(0, \mathbf{I}_{n_r})$ due to noise-whitening. Here, $(\mathbf{K}_n + \mathbf{K}_e)^{-\frac{1}{2}} = \mathbf{U} \Lambda^{-\frac{1}{2}} \mathbf{U}^H$. The equivalent signal model in (9) is similar to the one in (2) with the difference being a deterioration in the expected BMDR.

IV. BMDR PREDICTION

The result of Theorem 1 offers some insights into the error-probability behavior of a particular detector for a given set of channel matrix realizations. However, this is not particularly useful for choosing a particular channel coding scheme with exact CER guarantees because it is impossible to accurately estimate the channel matrices before observing them. *To be precise, $R_{\mathcal{D},i}(\mathcal{H}_{\mathcal{G}_i})$ is an achievable rate only if $\mathcal{H}_{\mathcal{G}_i}$ is known a priori or if the channel is static.* Nevertheless, the channel doesn't change drastically within a short instant of time for slow-moving users in an urban environment. Therefore, the result of Theorem 1 can be exploited for important tasks like link adaptation in a communication system. For any such task, it is vital to predict $R_{\mathcal{D},i}(\mathcal{H}_{\mathcal{G}_i})$ for a set of given channels $\mathcal{H}_{\mathcal{G}_i}$.

Unfortunately, the exact expression for $R_{\mathcal{D},i}(\mathbf{H}_{f,t})$ as given by (6) is not computable even for the simplest of linear detectors even though closed form expressions for $q_{\mathcal{D}}$ exist. However, $R_{\mathcal{D},i}(\mathbf{H}_{f,t})$ can be empirically approximated as follows. Let $\mathbf{s} \triangleq [\mathbf{s}_1^T, \mathbf{s}_2^T, \dots, \mathbf{s}_{N_u}^T]^T \in \mathcal{Q}^{N \times 1}$ with $\mathbf{s}_i \in \mathcal{Q}_i^{n_t^{(i)} \times 1}$ being complex random signal vectors whose realizations are the transmitted constellation signals chosen independently and uniformly from the constellation $\mathcal{Q}_i^{n_t^{(i)} \times 1}$, $i = 1, \dots, N_u$. It goes without saying that the bits $\{b_{f,t,i,l,j}\}$ also take values according to \mathbf{s}_i . Further, let $\mathbf{n} \in \mathbb{C}^{n_r \times 1}$ have the standard complex normal distribution. Therefore, by drawing N_{samp} independent samples of \mathbf{n} and \mathbf{s} , denoted respectively by $\{\mathbf{n}^{(r)}, r = 1, \dots, N_{\text{samp}}\}$ and $\{\mathbf{s}^{(r)}, r = 1, \dots, N_{\text{samp}}\}$, from their respective distributions, a Monte-Carlo approximation for (6) is given as

$$\bar{R}_{\mathcal{D},i}(\mathbf{H}_{f,t}) = 1 + \frac{1}{m_i n_t^{(i)} N_{\text{samp}}} \sum_{r=1}^{N_{\text{samp}}} \left\{ \sum_{l=1}^{n_t^{(i)}} \sum_{j=1}^{m_i} \log_2 \left(q_{\mathcal{D}}(b_{f,t,i,l,j}^{(r)}, \mathbf{y}^{(r)}, \mathbf{H}_{f,t}) \right) \right\} \quad (10)$$

where $\mathbf{y}^{(r)} = \mathbf{H}_{f,t} \mathbf{s}^{(r)} + \mathbf{n}^{(r)}$. $r = 1, \dots, N_{\text{samp}}$. From Hoeffding's inequality [24, Ch. 2], it follows that for all $\mathbf{H}_{f,t} \in \mathbb{C}^{n_r \times N}$

$$\mathbb{P} \left\{ \left| \bar{R}_{\mathcal{D},i}(\mathbf{H}_{f,t}) - R_{\mathcal{D},i}(\mathbf{H}_{f,t}) \right| \geq \delta \right\} \leq 2 \exp \left(-\frac{N_{\text{samp}}^2 \delta^2}{K} \right) \quad (11)$$

for any $\delta > 0$ with K being a positive constant dependent on L_{max} alone. Now, it would be of prohibitive complexity to perform a Monte-Carlo sampling to obtain the approximation in (10) for every observed channel in real time. Instead, the idea is to train a neural network that takes as input the channel realization $\mathbf{H}_{f,t}$ or some suitable function of $\mathbf{H}_{f,t}$, and outputs an estimate of $R_{\mathcal{D},i}(\mathbf{H}_{f,t})$. Let $f_{\Theta, \mathcal{D}, i}$ denote this neural network, with the set of trainable parameters denoted by Θ . Such a network would have to be trained on a dataset consisting of the labeled pairs $(g(\mathbf{H}), \bar{R}_{\mathcal{D},i}(\mathbf{H}))$, $\mathbf{H} \in \mathbb{C}^{n_r \times N}$ where g is some suitable function. Since the actual target label for a matrix $\mathbf{H}_{f,t}$ during training is $\bar{R}_{\mathcal{D},i}(\mathbf{H}_{f,t})$, we assume the following model for $f_{\Theta, \mathcal{D}, i}$:

$$f_{\Theta, \mathcal{D}, i}(g(\mathbf{H})) = \bar{R}_{\mathcal{D},i}(\mathbf{H}) + \varepsilon, \quad \mathbf{H} \in \mathbb{C}^{n_r \times N} \quad (12)$$

where ε is zero-mean bounded noise.

Remark 1. *Without using a machine-learning model, it is possible to estimate the BMDR of a linear detector for each user based on the post-equalization SINR. Such an equalization effectively creates N parallel channels (for the N transmitted symbols). By pre-computing (empirically) the BMDR for a SISO AWGN channel with maximum-likelihood decoding for every used constellation over a certain range of signal-to-noise ratios (SNRs), one can map the post-equalization SINR for each transmitted symbol in the MIMO setting to a BMDR value. Such an approach works very well for the LMMSE detector. So, a machine-learning model for BMDR prediction is only required for non-linear MU-MIMO detectors.*

V. TRAINING A CONVOLUTIONAL NEURAL NETWORK FOR BMDR PREDICTION

In this section, we describe a method to train a convolutional neural network (CNN) [25] to perform the prediction of $R_{\mathcal{D},i}(\mathbf{H})$ for a given channel $\mathbf{H} \in \mathbb{C}^{n_r \times N}$. Rewriting (2) and dropping the RE indices, we have

$$\mathbf{y} = \mathbf{H}\mathbf{s} + \mathbf{n} = \sum_{i=1}^{N_u} \sqrt{\frac{\rho_i}{n_t^{(i)}}} \mathbf{H}_i \mathbf{s}_i + \mathbf{n} \quad (13)$$

where $\mathbf{H}_i \in \mathbb{C}^{n_r \times n_t^{(i)}}$ has $\mathbb{E}_{\mathbf{H}_i} [\|\mathbf{H}_i\|^2] = n_r n_t^{(i)}$, $\mathbb{E}_{\mathbf{s}_i} [\mathbf{s}_i \mathbf{s}_i^H] = \mathbf{I}_{n_t^{(i)}}$, $\mathbf{n} \sim \mathcal{CN}(0, \mathbf{I}_{n_r})$, and ρ_i denotes the transmit power by UE i . Equivalently, following the definition in (1), we have the following model in the real domain.

$$\mathbf{y}^{\mathcal{R}} = \mathbf{H}^{\mathcal{R}} \mathbf{s}^{\mathcal{R}} + \mathbf{n}^{\mathcal{R}} \quad (14)$$

with $\mathbf{y}^{\mathcal{R}} \in \mathbb{R}^{2n_r \times 1}$, $\mathbf{n}^{\mathcal{R}} \sim \mathcal{N}(0, 0.5 \mathbf{I}_{2n_r})$, $\mathbf{s}^{\mathcal{R}} \in \mathbb{R}^{2N \times 1}$, and $\mathbf{H}^{\mathcal{R}} \in \mathbb{R}^{2n_r \times 2N}$. Upon the QR-decomposition of $\mathbf{H}^{\mathcal{R}}$, we obtain $\mathbf{H}^{\mathcal{R}} = \mathbf{Q}\mathbf{R}$ where $\mathbf{Q} \in \mathbb{R}^{2n_r \times 2N}$ is column orthogonal, and $\mathbf{R} \in \mathbb{R}^{2N \times 2N}$ is upper-triangular. A linear post-processing performed by left-multiplying $\mathbf{y}^{\mathcal{R}}$ by \mathbf{Q}^T results in

$$\bar{\mathbf{y}} \triangleq \mathbf{Q}^T \mathbf{y}^{\mathcal{R}} = \mathbf{R} \mathbf{s}^{\mathcal{R}} + \bar{\mathbf{n}} \quad (15)$$

where $\bar{\mathbf{y}} \in \mathbb{R}^{2N \times 1}$, and $\bar{\mathbf{n}} \triangleq \mathbf{Q}^T \mathbf{n}^{\mathcal{R}} \sim \mathcal{N}(0, 0.5 \mathbf{I}_{2N})$. Clearly, $R_{\mathcal{D},i}(\mathbf{H}) = R_{\mathcal{D},i}(\mathbf{R})$ for any detector \mathcal{D} and UE i , where $R_{\mathcal{D},i}(\mathbf{R})$ is computed in the real-domain. But since $N < n_r$, \mathbf{R} has less non-zero entries than \mathbf{H} , and also captures all the useful information pertaining to the BMDR in the following manner:

- 1) The upper off-diagonal elements capture the amount of inter-symbol interference (ISI) between users' symbols in the same channel use. The stronger their magnitudes relative to the diagonal elements, the smaller the BMDR.
- 2) The magnitudes of all the non-zero elements capture the SNR which influences the BMDR.

In essence, $R_{\mathcal{D},i}(\mathbf{H})$ is completely determined by the upper-triangular matrix \mathbf{R} when the other parameters n_r , $\{n_t^{(i)}, \mathcal{Q}_i\}_{i=1}^{N_u}$ are fixed. Therefore, we choose $g(\mathbf{H}) = \mathbf{R}$, where g is the function mentioned in (12). Note that other functions like the lower-triangular matrix from the QL-decomposition are also possible. The fact that QR-decomposition is also used in most sphere-decoding variants is the primary reason for our choice of g . Also, assuming that the used constellations are symmetric about the origin (as is the case with QAM), we have

$$R_{\mathcal{D},i}(\mathbf{R}) = R_{\mathcal{D},i}(\mathbf{R}\mathbf{D}) \quad (16)$$

where \mathbf{D} is any $2N \times 2N$ sized diagonal matrix with the diagonal elements being ± 1 . From (15), it follows that for any orthogonal matrix $\mathbf{U} \in \mathbb{R}^{2N \times 2N}$, we have $R_{\mathcal{D},i}(\mathbf{R}) = R_{\mathcal{D},i}(\mathbf{U}\mathbf{R})$. The only class of real-valued orthogonal matrices for which $\mathbf{U}\mathbf{R}$ continues to be upper-triangular is that of diagonal matrices with ± 1 entries. So, we have

$$R_{\mathcal{D},i}(\mathbf{R}) = R_{\mathcal{D},i}(\mathbf{D}\mathbf{R}) \quad (17)$$

Algorithm 1 Pseudocode to generate labeled data for a detector \mathcal{D} in a MU-MIMO system with n_r Rx antennas, N_u users; UE i has $n_t^{(i)}$ Tx antennas and uses a unit-energy constellation \mathcal{Q}_i with $|\mathcal{Q}_i| = m_i$. The minimum and maximum transmit power for UE i are $\rho_{min,i}$ and $\rho_{max,i}$ dB, respectively. Each channel matrix in the dataset generates N_p input feature-label pairs.

Input

\mathcal{H} : Set of composite MU-MIMO channel matrices of size $n_r \times N$, $N = \sum_{i=1}^{N_u} n_t^{(i)}$

Output

$\mathcal{X}_{L,\mathcal{D}}$: Set of input features

$\mathcal{Y}_{L,\mathcal{D}}^{(i)}$: Set of target labels for UE i with a one-to-one mapping to $\mathcal{X}_{L,\mathcal{D}}$

Initialize

$\mathcal{X}_{L,\mathcal{D}} \leftarrow \{\}, \mathcal{Y}_{L,\mathcal{D}}^{(i)} \leftarrow \{\}, \forall i = 1, \dots, N_u$

for all $\mathbf{H} = [\mathbf{H}_1, \dots, \mathbf{H}_{N_u}] \in \mathcal{H}$ **do**

$\mathbf{H}_{norm,i} \leftarrow \sqrt{n_r n_t^{(i)}} \mathbf{H}_i / \|\mathbf{H}_i\|, \forall i = 1, \dots, N_u, \mathbf{H}_{norm} \leftarrow [\mathbf{H}_{norm,1}, \dots, \mathbf{H}_{norm,N_u}]$

$\mathbf{Q}, \mathbf{R} \leftarrow \text{QR}(\mathbf{H}_{norm}^{\mathcal{R}})$ \triangleright QR-decomposition

for $k \leftarrow 1$ to N_p **do**

$\rho_{i,dB} \leftarrow \text{Sample}(\mathcal{U}([\rho_{min,i}, \rho_{max,i}])), \rho_i \leftarrow 10^{\rho_{i,dB}/10}, \forall i = 1, \dots, N_u$

$r_{\mathcal{D},i} \leftarrow 0, \forall i = 1, \dots, N_u$

for $t \leftarrow 1$ to N_{samp} **do**

$\mathbf{n} \leftarrow \text{Sample}(\mathcal{CN}(0, \mathbf{I}_{n_r}))$

for $i \leftarrow 1$ to N_u **do**

$b_{i,l,j} \leftarrow \text{Sample}(\mathcal{U}(\{0, 1\})), \forall l = 1, \dots, n_t^{(i)}, \forall j = 1, \dots, m_i$

$s_{i,l} \leftarrow \text{MAP}\{(b_{i,l,1}, \dots, b_{i,l,m_i}); \mathcal{Q}_i\}, \forall l = 1, \dots, n_t^{(i)}$

$\mathbf{s}_i \leftarrow [s_{i,1}, \dots, s_{i,n_t^{(i)}}]^T$

end for

$\mathbf{y} \leftarrow \sum_{i=1}^{N_u} \sqrt{\frac{\rho_i}{n_t^{(i)}}} \mathbf{H}_{norm,i} \mathbf{s}_i + \mathbf{n}, \Omega \leftarrow \text{diag}\left(\sqrt{\frac{\rho_1}{n_t^{(1)}}} \mathbf{I}_{n_t^{(1)}}, \dots, \sqrt{\frac{\rho_{N_u}}{n_t^{(N_u)}}} \mathbf{I}_{n_t^{(N_u)}}\right)$

$r_{\mathcal{D},i} \leftarrow r_{\mathcal{D},i} + \frac{\sum_{l=1}^{n_t^{(i)}} \sum_{j=1}^{m_i} \log_2(q_{\mathcal{D},i,l,j}(b_{i,l,j}; \mathbf{y}, \mathbf{H}_{norm} \Omega))}{m_i n_t^{(i)} N_{samp}}, \forall i = 1, \dots, N_u$

end for

$\bar{R}_{\mathcal{D},i} \leftarrow \max\{0, 1 + r_{\mathcal{D},i}\}, \forall i = 1, \dots, N_u$

$\mathcal{X}_{L,\mathcal{D}} \leftarrow \mathcal{X}_{L,\mathcal{D}} \cup \{\mathbf{R} \Omega^{\mathcal{R}}\}, \mathcal{Y}_{L,\mathcal{D}}^{(i)} \leftarrow \mathcal{Y}_{L,\mathcal{D}}^{(i)} \cup \{\bar{R}_{\mathcal{D},i}\}, \forall i = 1, \dots, N_u$

end for

end for

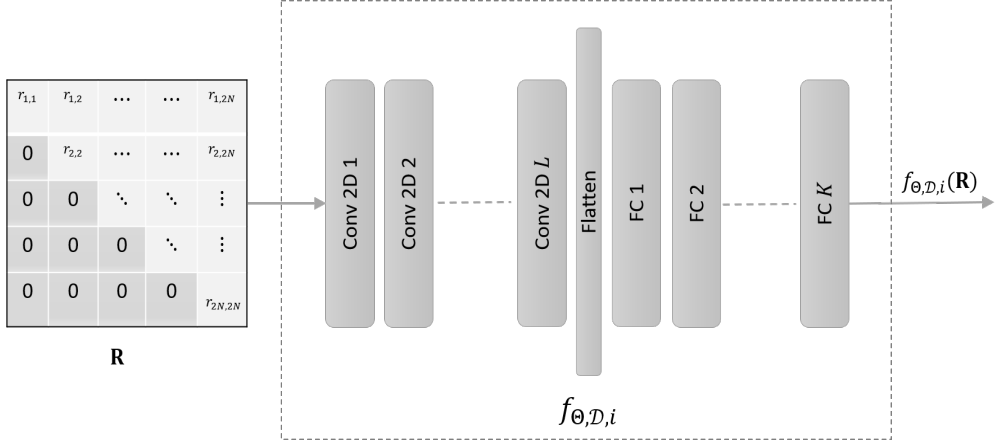


Fig. 3: A general CNN architecture for BMDR prediction with L convolutional (Conv2D) layers and K fully-connected (FC) layers.

where \mathbf{D} is a $2N \times 2N$ sized diagonal matrix with the diagonal elements being ± 1 . These facts will be utilized during the training process for data augmentation, mainly to increase the robustness of training and also for increased speed of convergence.

Algorithm 1 presents pseudocode to generate labeled data from a set of raw channels \mathcal{H} . In the algorithm, N_{samp} is the number of samples used for Monte-Carlo approximation. Note that for each channel matrix \mathbf{H} , we empirically calculate $\bar{R}_{\mathcal{D},i}(\mathbf{H})$ given by (10) for a detector \mathcal{D} and UE i , and store $\max\{0, \bar{R}_{\mathcal{D},i}(\mathbf{H})\}$. The BMDR approximations are computed over a set of useful transmit power values for each user.

We use a CNN for the purpose of BMDR prediction. This is motivated by the belief that a CNN has the ability to accurately identify the BMDR-defining patterns in the \mathbf{R} -matrix. Fig. 3 shows a general architecture of a simple CNN used for our purpose. Assuming the signal model given by (13), the input to the CNN will be \mathbf{R} where $\mathbf{R} \in \mathbb{R}^{2N \times 2N}$ is obtained by the QR-decomposition of $\mathbf{H}^{\mathcal{R}} \in \mathbb{R}^{2n_r \times 2N}$. The pseudocode for training the CNN is outlined in Algorithm 2. As mentioned earlier, the observations in (16) and (17) are exploited for data-augmentation in order to increase the robustness of the trained model. The model in (12) indicates that the noise ε is bounded, and within the bounded interval, the simulation results (see Figures 4 and 5 in Section VI) suggest that this noise is better approximated by a Laplacian random variable than a Gaussian one. Therefore, when the dataset does not have any zero-valued target labels, for any single label y_{true} and the corresponding predicted output y_{pred} , the loss function that we

Algorithm 2 Pseudocode for training a CNN to perform BMDR estimation for a detector \mathcal{D} and UE i , $i = 1, \dots, N_u$

Input

\mathcal{X}_{train} : Set of n_{train} input features; is a subset of $\mathcal{X}_{L,\mathcal{D}}$ obtained in Algorithm 1

\mathcal{Y}_{train} : Set of n_{train} labels corresponding to \mathcal{X}_{train} ; is a subset of $\mathcal{Y}_{L,\mathcal{D}}^{(i)}$

Output

$f_{\Theta^*,\mathcal{D},i}$: A trained CNN with parameters Θ^* that predicts $R_{\mathcal{D},i}(\mathbf{H})$ given by (6) for an input $\mathbf{R} \in \mathbb{R}^{2N \times 2N}$, the R-matrix of the QR-decomposition of $\mathbf{H}^{\mathcal{R}}$

Initialize

$\theta \leftarrow \theta_{init}$, $\forall \theta \in \Theta$

$\mathbb{D} \leftarrow \left\{ \left(\mathbf{R}^{(n)}, \bar{R}_{\mathcal{D},i}^{(n)} \right) \middle| \mathbf{R}^{(n)} \in \mathcal{X}_{train}, \bar{R}_{\mathcal{D},i}^{(n)} \in \mathcal{Y}_{train} \right\}_{n=1}^{n_{train}}$ \triangleright Dataset of labeled pairs

while Stopping Criteria *not reached* **do**

$\{\mathbb{D}_r\}_{r=1}^B \leftarrow \text{MiniBatch}(\mathbb{D})$ \triangleright Create B random mini-batches

for $r \leftarrow 1$ to B **do**

for all $\left(\mathbf{R}^{(n)}, \bar{R}_{\mathcal{D},i}^{(n)} \right) \in \mathbb{D}_r$ **do**

$\mathcal{L}_{\Theta,n}^{(1)} \leftarrow \text{Loss} \left(\bar{R}_{\mathcal{D},i}^{(n)}, f_{\Theta,\mathcal{D},i} \left(\mathbf{R}^{(n)} \right) \right)$

$d_k \leftarrow \text{Sample}(\mathcal{U}(\{-1, 1\})), \forall k = 1, \dots, 2N.$

$\mathbf{D} \leftarrow \text{diag}(d_1, \dots, d_{2N})$

\triangleright Data-Augmentation

$\mathcal{L}_{\Theta,n}^{(2)} \leftarrow \text{Loss} \left(\bar{R}_{\mathcal{D},i}^{(n)}, f_{\Theta,\mathcal{D},i} \left(\mathbf{R}^{(n)} \mathbf{D} \right) \right)$

$d_k \leftarrow \text{Sample}(\mathcal{U}(\{-1, 1\})), \forall k = 1, \dots, 2N.$

$\mathbf{D} \leftarrow \text{diag}(d_1, \dots, d_{2N})$

\triangleright Data-Augmentation

$\mathcal{L}_{\Theta,n}^{(3)} \leftarrow \text{Loss} \left(\bar{R}_{\mathcal{D},i}^{(n)}, f_{\Theta,\mathcal{D},i} \left(\mathbf{D} \mathbf{R}^{(n)} \right) \right)$

end for

$\mathcal{L}_{\Theta} \leftarrow \frac{1}{3|\mathbb{D}_r|} \sum_{n=1}^{|\mathbb{D}_r|} \sum_{l=1}^3 \mathcal{L}_{\Theta,n}^{(l)}$

$\nabla \mathcal{L}_{\Theta} \leftarrow \text{Gradients}(\mathcal{L}_{\Theta})$

\triangleright Compute gradients w.r.t each $\theta \in \Theta$

$\Theta \leftarrow \text{GradientDescentUpdate}(\Theta, \nabla \mathcal{L}_{\Theta})$

\triangleright Update Θ

end for

end while

choose in Algorithm 2 is given by

$$\text{Loss}(y_{true}, y_{pred}) = \frac{|y_{true} - y_{pred}|}{|y_{true}|} \quad (18)$$

so that the aggregated loss in a mini-batch is the *normalized mean absolute error*. Normalization aids in faster convergence. When the dataset has zero-valued target labels, we simply choose $\text{Loss}(y_{true}, y_{pred}) = |y_{true} - y_{pred}|$ for the entire dataset so that the aggregated loss in a mini-batch is the mean absolute error.

Note 1. *In MU-MIMO systems where the number of users served in each slot is variable, one can fix the maximum number of served users to be N_u^{\max} , and use Algorithm 1 to generate the labels by including $\rho_i = 0$ in the set of transmit powers levels for each $i = 1, \dots, N_u^{\max}$.*

Note 2. *For non-linear detectors which are invariant to user permutation, i.e., the LLR for each user is the same irrespective of the order of users, it is possible to use a single trained neural network for predicting the BMDR for each user. However, the input to the neural network in order to predict a particular user's BMDR needs to be the R-matrix of the appropriately permuted channel matrix.*

VI. SIMULATION RESULTS

In this section, we present our evaluation setup and some simulation results in support of our claims. We consider the 32-best detector as our choice of non-linear detector. Our reason for choosing $K = 32$ is that it is easy to implement. We would like to point out that in practice, $K = 64$ or higher is required for a significant improvement in performance compared to LMMSE.

A. Dataset and Training

A dataset of channel realizations was generated for the 3GPP 38.901 UMa NLoS [26, Sec. 7.2] scenario at a carrier frequency of 3.5 GHz using the QuaDRiGa channel simulator. We considered a BS equipped with a rectangular planar array consisting of 16 (2 vertical, 8 horizontal) single-polarized antennas installed at a height of 25 m with an antenna spacing of 0.5λ , where λ is the carrier wavelength. The BS was assumed to have a coverage angle of 120° and a coverage radius of 250 m. Within this coverage sector, the region within a distance of 25–250 m from the BS was considered for the random placement of four single-antenna users ($N_u = 4$). Once a user was dropped at a particular position, it was assumed to move along a linear trajectory with a

Layer	Channels/Neurons	Kernel size	Activation	Output Shape	Number of Parameters
Input Layer	N/A	N/A	N/A	$(B_S, 8, 8, 1)$	0
Conv2D 1	32	$(2, 2)$	ReLU	$(B_S, 8, 8, 32)$	160
Conv2D 2	16	$(2, 2)$	ReLU	$(B_S, 8, 8, 16)$	2064
Conv2D 3	8	$(2, 2)$	ReLU	$(B_S, 7, 7, 8)$	520
Flatten	N/A	N/A	N/A	$(B_S, 392)$	0
FC 1	8	N/A	ReLU	$(B_S, 8)$	3144
FC 2	4	N/A	ReLU	$(B_S, 4)$	36
FC 3	1	N/A	ReLU	$(B_S, 1)$	5

TABLE I: Architecture details of the CNN used for training, with a total of 5929 trainable parameters. Here B_S denotes the batch size.

speed varying between 18–35 kmph. Channels were sampled every 35.7 μ s to obtain sequences of length $N_{symb} = 70$ (corresponds to 5 slots of 14 symbols each in 5G NR). Each channel realization was then converted to the frequency domain assuming a bandwidth of 2.16 MHz and $N_{sc} = 72$ sub-carriers with a subcarrier spacing of 30 kHz, i.e., 6 physical resource blocks (PRBs) in 5G NR. A total of $N_{drops} = 400$ independent user drops were obtained, resulting in $400 * 70 * 72 = 2.016$ million channel matrices of size 16×4 arranged as an array of dimensions $(400, 72, 70, 16, 4)$ (to be read as $(N_{drops}, N_{sc}, N_{symb}, n_r, N_u)$). Since the path-loss can vary dramatically between different users, we assumed perfect power control per sequence of 70 symbols so that

$$\frac{1}{70N_{sc}} \sum_{f=1}^{N_{sc}} \sum_{t=1}^{70} \left\| \mathbf{h}_{f,t}^{(i)} \right\|^2 = 16, \quad \forall i = 1, 2, 3, 4, \quad (19)$$

where $\mathbf{h}_{f,t}^{(i)}$ is the channel from UE i to the BS on subcarrier f and symbol t . From the resulting set of matrices, we chose a set \mathcal{H} of 10,000 matrices with condition numbers uniformly distributed between 0–25 dB. For this set of channel matrices, a training dataset was generated for the 32-best detector as described in Algorithm 1 with $N_{samp} = 500$ and $N_p = 50$, resulting in 500,000 feature-label pairs. The set of randomly sampled transmit powers (in dB) was taken to be from the set $[-16, -6]$, $[-8, 0]$, and $[-4, 10]$, respectively, for 4/16/64–QAM. In total, there are $3^4 = 81$ combinations of user constellations and 500,000 feature-label pairs for each of them. A test dataset was generated similarly for a separate set of 5,000 channel matrices.

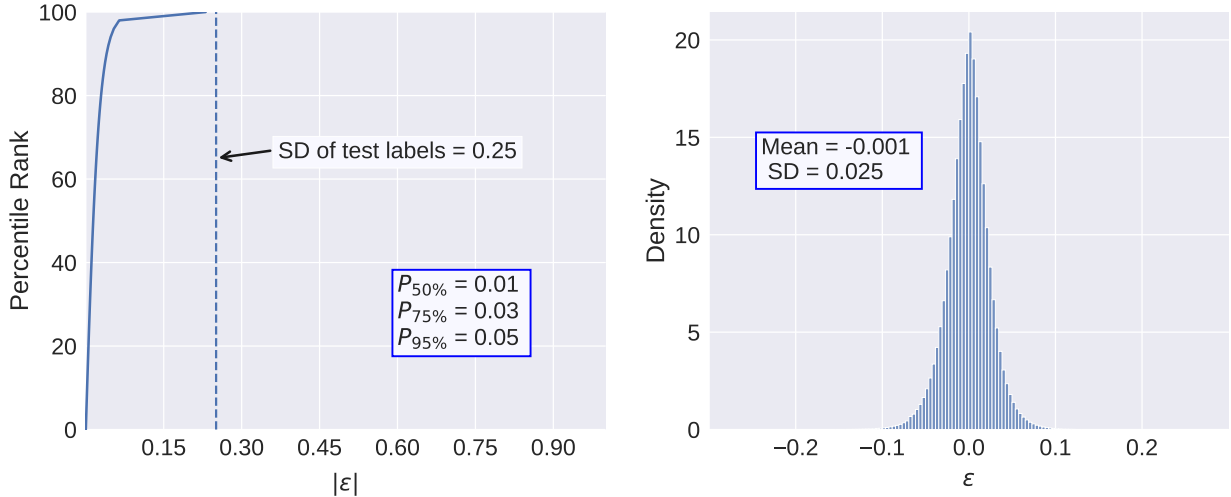


Fig. 4: The percentiles of the absolute value of the LMMSE BMDR prediction error (left) and the error histogram (right).

Table I details the architecture of the CNN that was trained using Algorithm 2 to predict BMDR for the 32-best detector.

B. Numerical Results

We used the trained CNN to predict the BMDR on the test data with 250,000 feature-label pairs for each of the 81 combinations of QAM constellations for the four users. As for the LMMSE detector, the labels were generated as explained in Algorithm 1, but the prediction was performed as explained in Remark 1.

Figure 4 shows the plot of the percentile ranks (left plot) of the absolute value of the prediction error, i.e., $|\varepsilon|$ for ε as given in (12), and the histogram of ε on the right. The percentiles here refer to the percentage of test predictions that have absolute errors less than any given $|\varepsilon|$ on the X-axis. The standard deviation (SD) of the test labels is 0.25, while the SD of the prediction error is 0.025. The corresponding plots for the 32-best detector are shown in Fig. 5. In both the figures, the 50th, 75th, and the 95th percentiles for $|\varepsilon|$ are highlighted. The accuracy of prediction for the 32-best detector is slightly worse compared to that of the LMMSE detector. This is expected, since a non-linear detector will exhibit more variations in BMDR compared to a linear detector for the same amount of perturbation in the channel coefficients.

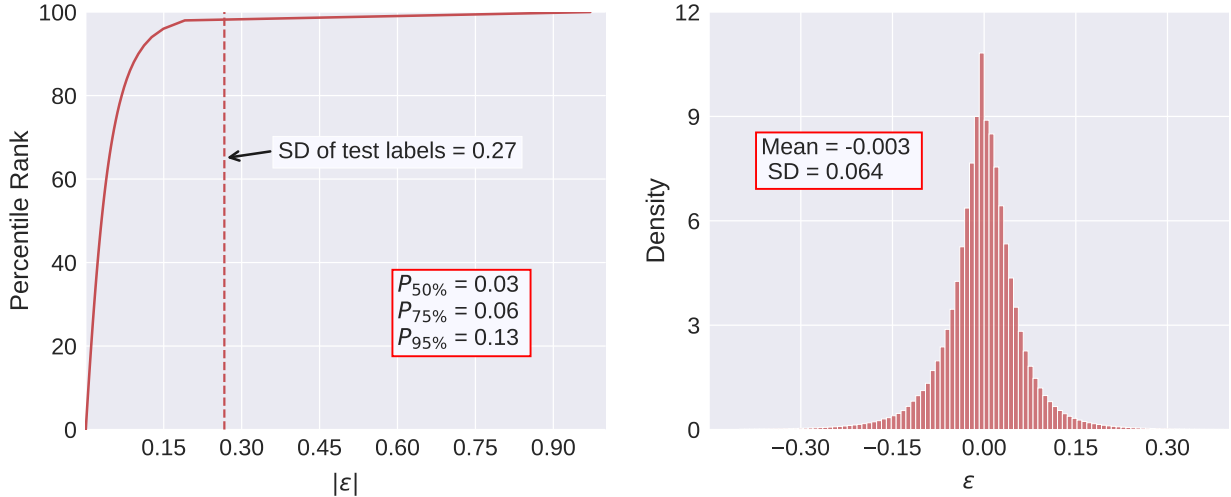


Fig. 5: The percentiles of the absolute value of the 32-best BMDR prediction error (left) and the error histogram (right).

Sequence length	50 th percentile		75 th percentile		95 th percentile	
	LMMSE	32-best	LMMSE	32-best	LMMSE	32-best
10	0.005	0.013	0.008	0.026	0.018	0.072
50	0.002	0.008	0.004	0.016	0.008	0.043
100	0.002	0.008	0.003	0.015	0.006	0.039

TABLE II: Statistics for the absolute error with averaging over different sequence lengths.

In real-world applications, we do not actually rely on BMDR prediction for one channel realization, but rather on a sequence of channel realizations over which the codeword bits are transmitted. Therefore, we are more interested in the BMDR-prediction errors for sequences of channel realizations. In view of this, we consider sequences of channel realizations in the test dataset, each sequence consisting of channel realizations for consecutive REs in frequency. We consider sequences of length 10, 50, and 100, with the start of the sequence being arbitrary. For each sequence length, we consider 20,000 sequences, and record the prediction error of the BMDR average for each sequence. The percentiles of this error are plotted in Fig. 6 for both the detectors, and Table II displays the 50th, 75th and the 95th percentile for each case. It can be seen that the mean prediction error with averaging is quite low even for the 32-best detector, and this is promising from the perspective of both LA and PHY abstraction.

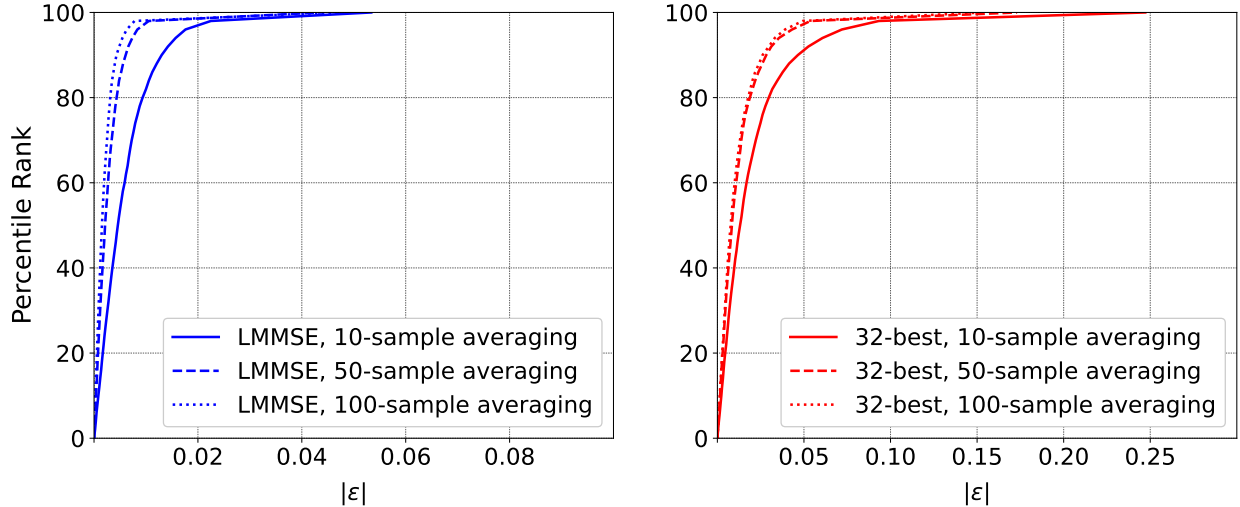


Fig. 6: The percentiles of the absolute error with averaging over different sequence lengths for LMMSE (left) and 32-best (right).

VII. DISCUSSION AND CONCLUDING REMARKS

For MU-MIMO systems with non-linear receivers, LA and PHY abstraction are quite challenging to perform due to the absence of a suitable metric that is equivalent to post-equalization SINR in linear receivers. In this paper, we introduced BMDR of a detector as one such equivalent metric. The relationship between BMDR, transmission code-rate, and CER for a detector was established, and a method to estimate the BMDR using a trained CNN was presented. Simulation results were provided to substantiate our claims.

While the training process itself is quick and the objective of BMDR prediction can be achieved with relatively simple CNN models, the task that involves the highest amount of computational resources (though offline only) is the preparation of labeled data. For every MU-MIMO configuration, defined by the number of receive antennas n_r , number of users N_u , number of transmit antennas $n_t^{(i)}$ for UE i , and constellation \mathcal{Q}_i for UE i , one needs to prepare labeled data. So, this would probably limit the usage of the proposed technique to relatively smaller MU-MIMO configurations. In the next part of this paper, the concepts developed thus far will be further exploited to perform LA and PHY abstraction for both linear and non-linear MU-MIMO receivers.

APPENDIX

Proof of Theorem 1

To prove the existence of such a code, we take the following steps which are similar to those of [20] and [27], even though the setting is different. We make use of the random coding argument. Let $\mathcal{E}_{i,j}(w)$ denote the j^{th} bit of the codeword $\mathcal{E}_i(w)$ for the i^{th} user's message w . The codewords are generated by independently and uniformly drawing bits so that $\forall w \in \mathcal{W}_i$, $\mathbb{P}\{\mathcal{E}_{i,j}(w) = 0\} = \mathbb{P}\{\mathcal{E}_{i,j}(w) = 1\}$, $\forall j = 1, \dots, n_i$. Once the codebook \mathcal{C}_i is generated, it is revealed to the receiver. For convenience, we drop the explicit mention of the cardinality of $\mathcal{G}_i(n_i/(m_i n_t^{(i)}))$ and simply use the notation \mathcal{G}_i . We also do not explicitly mention the involvement of the interleaver. As mentioned before, the realizations of the received signal vectors and the channel matrices are $\mathbf{y}_{f,t}$ and $\mathbf{H}_{f,t}$ respectively. At the receiver side, the transmitted message is estimated to be \hat{w} and is given as

$$\hat{w} = \arg \max_{w \in \mathcal{W}_i} \left(\underbrace{\prod_{(f,t) \in \mathcal{G}_i} \prod_{l=1}^{n_t^{(i)}} \prod_{j=1}^{m_i} q_{\mathcal{D}}(b_{f,t,i,l,j}(w); \mathbf{y}_{f,t}, \mathbf{H}_{f,t})}_{\triangleq \bar{q}_{\mathcal{D}}(\mathcal{E}_i(w); \mathcal{Y}_{\mathcal{G}_i}, \mathcal{H}_{\mathcal{G}_i})} \right). \quad (20)$$

Let E denote the codeword error event. We are interested in $\mathbb{P}\{E | \mathcal{H}_{\mathcal{G}_i} = \mathcal{H}_{\mathcal{G}_i}\}$. Suppose that a message w was transmitted. Then,

$$\mathbb{P}\{E | \mathcal{E}_i(w), \mathcal{H}_{\mathcal{G}_i} = \mathcal{H}_{\mathcal{G}_i}\} = \mathbb{E}_{\mathcal{Y}_{\mathcal{G}_i}} [\mathbb{P}\{E | \mathcal{E}_i(w), \mathcal{Y}_{\mathcal{G}_i} = \mathcal{Y}_{\mathcal{G}_i}, \mathcal{H}_{\mathcal{G}_i} = \mathcal{H}_{\mathcal{G}_i}\}] \quad (21)$$

$$= \mathbb{E}_{\mathcal{Y}_{\mathcal{G}_i}} \left[\mathbb{P} \left\{ \bigcup_{w' \neq w} [\bar{q}_{\mathcal{D}}(\mathcal{E}(w'); \mathcal{Y}_{\mathcal{G}_i}, \mathcal{H}_{\mathcal{G}_i}) \geq \bar{q}_{\mathcal{D}}(\mathcal{E}_i(w); \mathcal{Y}_{\mathcal{G}_i}, \mathcal{H}_{\mathcal{G}_i})] \middle| \begin{array}{l} \mathcal{Y}_{\mathcal{G}_i} = \mathcal{Y}_{\mathcal{G}_i}, \quad \mathcal{E}_i(w), \\ \mathcal{H}_{\mathcal{G}_i} = \mathcal{H}_{\mathcal{G}_i} \end{array} \right\} \right] \quad (22)$$

$$\leq \mathbb{E}_{\mathcal{Y}_{\mathcal{G}_i}} \left[\mathbb{P} \left\{ \sum_{w' \neq w} [\bar{q}_{\mathcal{D}}(\mathcal{E}(w'); \mathcal{Y}_{\mathcal{G}_i}, \mathcal{H}_{\mathcal{G}_i}) \geq \bar{q}_{\mathcal{D}}(\mathcal{E}_i(w); \mathcal{Y}_{\mathcal{G}_i}, \mathcal{H}_{\mathcal{G}_i})] \middle| \begin{array}{l} \mathcal{Y}_{\mathcal{G}_i} = \mathcal{Y}_{\mathcal{G}_i}, \quad \mathcal{E}_i(w), \\ \mathcal{H}_{\mathcal{G}_i} = \mathcal{H}_{\mathcal{G}_i} \end{array} \right\} \right] \quad (23)$$

where (23) is due to the union bound. Now, given that $\mathcal{E}_i(w)$ was transmitted and $\mathcal{H}_{\mathcal{G}_i}, \mathcal{Y}_{\mathcal{G}_i}$ were observed, $\bar{q}_{\mathcal{D}}(\mathcal{E}_i(w); \mathcal{Y}_{\mathcal{G}_i}, \mathcal{H}_{\mathcal{G}_i})$ is deterministic. However, $\bar{q}_{\mathcal{D}}(\mathcal{E}(w'); \mathcal{Y}_{\mathcal{G}_i}, \mathcal{H}_{\mathcal{G}_i})$ is a random variable due to the randomness of the code construction. Therefore, applying the Markov inequality, we have

$$\mathbb{P}\{E | \mathcal{E}_i(w), \mathcal{H}_{\mathcal{G}_i} = \mathcal{H}_{\mathcal{G}_i}\} \quad (24)$$

$$\leq \mathbb{E}_{\mathcal{Y}_{\mathcal{G}_i}} \left[\frac{1}{\bar{q}_{\mathcal{D}}(\mathcal{E}_i(w); \mathcal{Y}_{\mathcal{G}_i}, \mathcal{H}_{\mathcal{G}_i})} \sum_{w' \neq w} \mathbb{E}_{\mathcal{E}} [\bar{q}_{\mathcal{D}}(\mathcal{E}(w'); \mathcal{Y}_{\mathcal{G}_i}, \mathcal{H}_{\mathcal{G}_i})] \middle| \mathcal{E}_i(w), \mathcal{Y}_{\mathcal{G}_i} = \mathcal{Y}_{\mathcal{G}_i}, \mathcal{H}_{\mathcal{G}_i} = \mathcal{H}_{\mathcal{G}_i} \right]$$

where $\mathbb{E}_{\mathcal{E}}[\cdot]$ implies that the expectation is over the randomness of the codeword generation process. Therefore, we have

$$\mathbb{P}\{E|\mathcal{E}_i(w), \mathcal{H}_{\mathcal{G}_i} = \mathcal{H}_{\mathcal{G}_i}\} \leq \mathbb{E}_{\mathcal{Y}_{\mathcal{G}_i}} \left[\frac{2^{k_i}}{\bar{q}_{\mathcal{D}}(\mathcal{E}_i(w); \mathcal{Y}_{\mathcal{G}_i}, \mathcal{H}_{\mathcal{G}_i})} \mathbb{E}_{\mathcal{E}}[\bar{q}_{\mathcal{D}}(\mathcal{E}(w'); \mathcal{Y}_{\mathcal{G}_i}, \mathcal{H}_{\mathcal{G}_i})] \middle| \mathcal{E}_i(w), \mathcal{Y}_{\mathcal{G}_i} = \mathcal{Y}_{\mathcal{G}_i}, \mathcal{H}_{\mathcal{G}_i} = \mathcal{H}_{\mathcal{G}_i} \right] \quad (25)$$

$$= \mathbb{E}_{\mathcal{Y}_{\mathcal{G}_i}} \left[\frac{2^{k_i} \prod_{(f,t) \in \mathcal{G}_i} \prod_{l=1}^{n_t^{(i)}} \prod_{j=1}^{m_i} \mathbb{E}_{b_{f,t,i,l,j}} [q_{\mathcal{D}}(b_{f,t,i,l,j}(w'); \mathbf{y}_{f,t}, \mathbf{H}_{f,t})]}{\prod_{(f,t) \in \mathcal{G}_i} \prod_{l=1}^{n_t^{(i)}} \prod_{j=1}^{m_i} q_{\mathcal{D}}(b_{f,t,i,l,j}(w); \mathbf{y}_{f,t}, \mathbf{H}_{f,t})} \middle| \mathcal{Y}_{\mathcal{G}_i} = \mathcal{Y}_{\mathcal{G}_i}, \mathcal{E}_i(w), \mathcal{H}_{\mathcal{G}_i} = \mathcal{H}_{\mathcal{G}_i} \right] \quad (26)$$

$$= \mathbb{E}_{\mathcal{Y}_{\mathcal{G}_i}} \left[\frac{2^{k_i - n_i}}{\prod_{(f,t) \in \mathcal{G}_i} \prod_{l=1}^{n_t^{(i)}} \prod_{j=1}^{m_i} q_{\mathcal{D}}(b_{f,t,i,l,j}(w); \mathbf{y}_{f,t}, \mathbf{H}_{f,t})} \middle| \mathcal{E}_i(w), \mathcal{Y}_{\mathcal{G}_i} = \mathcal{Y}_{\mathcal{G}_i}, \mathcal{H}_{\mathcal{G}_i} = \mathcal{H}_{\mathcal{G}_i} \right] \quad (27)$$

where (25) is because of the codewords are independently and identically generated, (26) is because the code bits of every codeword are independently drawn, (27) is because the code bits are uniformly drawn and $q_{\mathcal{D}}(\cdot)$ forms a probability mass function. With $R_{\mathcal{C}_i} = k_i/n_i$, we have from (27)

$$\mathbb{P}\{E|\mathcal{H}_{\mathcal{G}_i} = \mathcal{H}_{\mathcal{G}_i}\} \leq \mathbb{E}_{w, \mathcal{Y}_{\mathcal{G}_i}} \left[2^{-n_i \left[1 + \frac{\sum_{(f,t) \in \mathcal{G}_i} \sum_{l=1}^{n_t^{(i)}} \sum_{j=1}^{m_i} \log_2(q_{\mathcal{D}}(b_{f,t,i,l,j}(w); \mathbf{y}_{f,t}, \mathbf{H}_{f,t}))}{n_i} - R_{\mathcal{C}_i} \right]} \middle| \mathcal{Y}_{\mathcal{G}_i} = \mathcal{Y}_{\mathcal{G}_i}, \mathcal{E}_i(w), \mathcal{H}_{\mathcal{G}_i} = \mathcal{H}_{\mathcal{G}_i} \right]. \quad (28)$$

Consider the quantity

$$X_{f,t} \triangleq \frac{1}{n_i} \sum_{l=1}^{n_t^{(i)}} \sum_{j=1}^{m_i} \log_2(q_{\mathcal{D}}(b_{f,t,i,l,j}; \mathbf{y}_{f,t}, \mathbf{H}_{f,t})). \quad (29)$$

It can be noted that $X_{f,t}$ is a random function of three random entities: $\mathbf{s}_{f,t}$, $\mathbf{n}_{f,t}$, and $\mathbf{H}_{f,t}$, with $b_{f,t,i,l,j}$ themselves having a bijective map with the appropriate elements of $\mathbf{s}_{f,t}$. The $\mathbf{y}_{f,t}$ are independent of one another for different values of (f,t) due to the independence of $\mathbf{n}_{f,t}$. This implies that the $X_{f,t}$ are independent random variables. If the $\mathbf{H}_{f,t}$ came from a stationary distribution, we could have considered the expectation of $X_{f,t}$ over $\mathbf{H}_{f,t}$ for the rest of the proof. However, we do not make any such assumption on the stationarity of the random channel matrices, and this is justified in a practical wireless environment. Therefore, we proceed by conditioning on the channel matrix realizations.

From the assumption in (5), we have $-m_i n_t^{(i)} C / n_i < X_{f,t} < 0, \forall (f,t) \in \mathcal{G}_i$ with $C = \log_2(e) L_{max} + 1$, and the $X_{f,t}$ are independent random variables conditioned on $\mathcal{H}_{\mathcal{G}_i} = \mathcal{H}_{\mathcal{G}_i}$. From Hoeffding's inequality, we have for any $\delta > 0$,

$$\mathbb{P} \left\{ \sum_{(f,t) \in \mathcal{G}_i} (X_{f,t} | \mathbf{H}_{f,t} = \mathbf{H}_{f,t}) < \sum_{(f,t) \in \mathcal{G}_i} \mathbb{E}_{\mathbf{y}_{f,t} | \mathbf{H}_{f,t}} [X_{f,t} | \mathbf{H}_{f,t} = \mathbf{H}_{f,t}] - \delta \right\} < \exp \left(-\frac{n_i \delta^2}{K} \right) \quad (30)$$

with $K = m_i n_t^{(i)} C^2 / 2$ being a positive constant independent of n_i . Let

$$\mathcal{A}(\mathcal{H}_{\mathcal{G}_i}) \triangleq \left\{ \mathbf{y}_{f,t}, \forall (f,t) \in \mathcal{G}_i \left| \sum_{(f,t) \in \mathcal{G}_i} (X_{f,t} | \mathcal{H}_{\mathcal{G}_i} = \mathcal{H}_{\mathcal{G}_i}) \geq \sum_{(f,t) \in \mathcal{G}_i} \mathbb{E}[X_{f,t} | \mathcal{H}_{\mathcal{G}_i} = \mathcal{H}_{\mathcal{G}_i}] - \delta \right. \right\} \quad (31)$$

and let $\mathcal{A}(\mathcal{H}_{\mathcal{G}_i})^c$ denote its complement. Then, using (30) in (28), we obtain

$$\begin{aligned} \mathbb{P}\{E | \mathcal{H}_{\mathcal{G}_i} = \mathcal{H}_{\mathcal{G}_i}\} &= \mathbb{E}_{w \in \mathcal{W}_i, \mathbf{y}_{\mathcal{G}_i}} [\mathbb{P}\{E, \mathcal{A}(\mathcal{H}_{\mathcal{G}_i}) | \mathcal{E}_i(w), \mathbf{y}_{\mathcal{G}_i} = \mathcal{Y}_{\mathcal{G}_i}, \mathcal{H}_{\mathcal{G}_i} = \mathcal{H}_{\mathcal{G}_i}\}] \\ &\quad + \mathbb{E}_{w \in \mathcal{W}_i, \mathbf{y}_{\mathcal{G}_i}} [\mathbb{P}\{E, \mathcal{A}(\mathcal{H}_{\mathcal{G}_i})^c | \mathcal{E}_i(w), \mathbf{y}_{\mathcal{G}_i} = \mathcal{Y}_{\mathcal{G}_i}, \mathcal{H}_{\mathcal{G}_i} = \mathcal{H}_{\mathcal{G}_i}\}] \end{aligned} \quad (32)$$

$$\leq 2^{-n_i(R_{\mathcal{D},i}(\mathcal{H}_{\mathcal{G}_i}) - \delta - R_{\mathcal{C}_i})} + e^{-\frac{n_i \delta^2}{K}}. \quad (33)$$

Therefore, for any $\epsilon \in (0, 1]$, by choosing n_i to be sufficiently large, the probability of codeword error can be made smaller than ϵ provided that $R_{\mathcal{C}_i}(n_i) < R_{\mathcal{D},i}^{min} - \delta$ for some $\delta \in (0, R_{\mathcal{D},i}^{min})$.

To prove the other part of the theorem, we proceed as follows. Due to the assumption that the bits comprising $\mathcal{B}_{f,t,i} = \{b_{f,t,i,l,j}\}$ are i.i.d., we have

$$I(\mathcal{B}_{f,t,i}; \mathbf{y}_{\mathcal{G}_i} | \mathcal{H}_{\mathcal{G}_i} = \mathcal{H}_{\mathcal{G}_i}) = \sum_{(f,t) \in \mathcal{G}_i} \sum_{j,l} I(b_{f,t,i,l,j}; \mathbf{y}_{f,t} | \mathbf{H}_{f,t} = \mathbf{H}_{f,t}) \quad (34)$$

where $I(X; Y)$ denotes the MI between random variables X and Y . For convenience, we drop the subscripts, and let $Q_D \triangleq q_{\mathcal{D}}(b; \mathbf{y}, \mathbf{H})$ denote the posterior distribution for bit b generated by \mathcal{D} for a channel realization \mathbf{H} . Now,

$$I(b; \mathbf{y}, Q_D | \mathbf{H} = \mathbf{H}) = I(b; \mathbf{y} | \mathbf{H} = \mathbf{H}) + I(b; Q_D | \mathbf{y}, \mathbf{H} = \mathbf{H}) \quad (35)$$

$$= I(b; Q_D | \mathbf{H} = \mathbf{H}) + I(b; \mathbf{y} | Q_D, \mathbf{H} = \mathbf{H}). \quad (36)$$

Since $Q_D = f(\mathbf{y})$ (for some function f , given a channel realization \mathbf{H}), we have $I(b; Q_D | \mathbf{y}, \mathbf{H}) = 0$, and so

$$I(b; Q_D | \mathbf{H} = \mathbf{H}) = I(b; \mathbf{y} | \mathbf{H} = \mathbf{H}) - I(b; \mathbf{y} | Q_D, \mathbf{H} = \mathbf{H}). \quad (37)$$

But, $I(b; \mathbf{y}|Q_D, \mathbf{H} = \mathbf{H}) = H(b|Q_D, \mathbf{H} = \mathbf{H}) - H(b|\mathbf{y}, Q_D, \mathbf{H} = \mathbf{H}) = H(b|Q_D, \mathbf{H} = \mathbf{H}) - H(b|\mathbf{y}, \mathbf{H} = \mathbf{H})$, where $H()$ denotes the binary entropy. Let $P(X, Y)$ denote the joint probability distribution function of random variables X and Y . Then,

$$H(b|Q_D, \mathbf{H} = \mathbf{H}) = - \int_{Q_D} \sum_b P(b, Q_D | \mathbf{H} = \mathbf{H}) \log_2 (P(b|Q_D, \mathbf{H} = \mathbf{H})) dQ_D \quad (38)$$

$$= - \int_{\mathbf{y}} \sum_b P(b, \mathbf{y} | \mathbf{H} = \mathbf{H}) \log_2 (P(b|\mathbf{y}, \mathbf{H} = \mathbf{H})) d\mathbf{y} \quad (39)$$

$$= -\mathbb{E}_{\mathbf{y}|\mathbf{H}} \left[\sum_b P(b|\mathbf{y}, \mathbf{H} = \mathbf{H}) \log_2 (Q_D) \right] \quad (40)$$

where (39) is due to a simple change of variables and $P(b|\mathbf{y}, \mathbf{H} = \mathbf{H})$ denotes the true posterior distribution of b conditioned on a channel realization \mathbf{H} . Further,

$$H(b|\mathbf{y}, \mathbf{H} = \mathbf{H}) = - \int_{\mathbf{y}} \sum_b P(b, \mathbf{y} | \mathbf{H} = \mathbf{H}) \log_2 (P(b|\mathbf{y}, \mathbf{H} = \mathbf{H})) d\mathbf{y} \quad (41)$$

$$= - \int_{\mathbf{y}} \sum_b P(b, \mathbf{y} | \mathbf{H} = \mathbf{H}) \log_2 (P(b|\mathbf{y}, \mathbf{H} = \mathbf{H})) d\mathbf{y} \quad (42)$$

$$= -\mathbb{E}_{\mathbf{y}|\mathbf{H}} \left[\sum_b P(b|\mathbf{y}, \mathbf{H} = \mathbf{H}) \log_2 (P(b|\mathbf{y}, \mathbf{H} = \mathbf{H})) \right]. \quad (43)$$

Therefore,

$$I(b; \mathbf{y}|Q_D, \mathbf{H} = \mathbf{H}) = \mathbb{E}_{\mathbf{y}|\mathbf{H}} [D_{KL}(P(b|\mathbf{y}, \mathbf{H} = \mathbf{H}) || q_{\mathcal{D}}(b; \mathbf{y}, \mathbf{H}))] \quad (44)$$

where $D_{KL}(p||q)$ denotes Kullback–Leibler (KL)-divergence between distributions p and q . A straightforward calculation shows that

$$I(b; \mathbf{y} | \mathbf{H} = \mathbf{H}) = H(b | \mathbf{H} = \mathbf{H}) - H(b | \mathbf{y}, \mathbf{H} = \mathbf{H}) \quad (45)$$

$$= 1 + \mathbb{E}_{\mathbf{y}|\mathbf{H}} \left[\sum_b P(b|\mathbf{y}, \mathbf{H} = \mathbf{H}) \log_2 (P(b|\mathbf{y}, \mathbf{H} = \mathbf{H})) \right]. \quad (46)$$

Using (46) and (44) in (37), and noting that $n_i = mn_t^{(i)}|\mathcal{G}_i|$, we obtain

$$I(\mathcal{B}_{f,t,i}; Q_D(\mathcal{B}_{f,t,i}) | \mathcal{H}_{\mathcal{G}_i} = \mathcal{H}_{\mathcal{G}_i}) = \sum_{(f,t) \in \mathcal{G}_i} \sum_{j,l} I(b_{f,t,i,l,j}; Q_D(b_{f,t,i,l,j}) | \mathbf{H}_{f,t} = \mathbf{H}_{f,t}) \quad (47)$$

$$= n_i R_{\mathcal{D},i}(\mathcal{H}_{\mathcal{G}_i}). \quad (48)$$

Therefore, $R_{\mathcal{D},i}(\mathcal{H}_{\mathcal{G}_i})$ represents the normalized (by the codeword length) mutual information between the transmitted bits and the detector output conditioned on a set of channel realizations $\mathcal{H}_{\mathcal{G}_i}$, and there exists no code which can transmit at a rate higher than it for reliable transmission.

REFERENCES

- [1] D. Tse and P. Viswanath, *Fundamentals of Wireless Communication*. USA: Cambridge University Press, 2005.
- [2] J. M. Cioffi, G. P. Dudevoir, M. Vedat Eyuboglu, and G. D. Forney, “MMSE Decision-Feedback Equalizers and Coding. I. Equalization Results,” *IEEE Trans. Commun.*, vol. 43, no. 10, pp. 2582–2594, 1995.
- [3] E. Viterbo and J. Boutros, “A Universal Lattice Code Decoder for Fading Channels,” *IEEE Trans. Inf. Theory*, vol. 45, no. 5, pp. 1639–1642, 1999.
- [4] C. Studer and H. Bölskei, “Soft–Input Soft–Output Single Tree-Search Sphere Decoding,” *IEEE Trans. Inf. Theory*, vol. 56, no. 10, pp. 4827–4842, 2010.
- [5] L. G. Barbero and J. S. Thompson, “Fixing the Complexity of the Sphere Decoder for MIMO Detection,” *IEEE Trans. Wireless Commun.*, vol. 7, no. 6, pp. 2131–2142, 2008.
- [6] Z. Guo and P. Nilsson, “Algorithm and Implementation of the K-best Sphere decoding for MIMO Detection,” *IEEE J. Sel. Areas Commun.*, vol. 24, no. 3, pp. 491–503, 2006.
- [7] W. J. Choi, K. W. Cheong, and J. M. Cioffi, “Iterative soft interference cancellation for multiple antenna systems,” in *IEEE Wireless Communications and Networking Conference. Conference Record (Cat. No.00TH8540)*, vol. 1, 2000, pp. 304–309.
- [8] M. Honkala, D. Korpi, and J. M. J. Huttunen, “Deeprx: Fully convolutional deep learning receiver,” *IEEE Transactions on Wireless Communications*, vol. 20, no. 6, pp. 3925–3940, 2021.
- [9] 3GPP, “NR; Multiplexing and channel coding,” 3rd Generation Partnership Project (3GPP), Technical Specification (TS) 38.212, 12 2020, version 16.4.0. [Online]. Available: <https://portal.3gpp.org/desktopmodules/Specifications/SpecificationDetails.aspx?specificationId=3214>
- [10] P. Bertrand, J. Jiang, and A. Ekpenyong, “Link Adaptation Control in LTE Uplink,” in *2012 IEEE Vehicular Technology Conference (VTC Fall)*, 2012, pp. 1–5.
- [11] M. G. Sarret, D. Catania, F. Frederiksen, A. F. Cattoni, G. Berardinelli, and P. Mogensen, “Dynamic Outer Loop Link Adaptation for the 5G Centimeter-Wave Concept,” in *Proceedings of European Wireless 2015; 21th European Wireless Conference*, 2015, pp. 1–6.
- [12] S. Sun, S. Moon, and J.-K. Fwu, “Practical Link Adaptation Algorithm With Power Density Offsets for 5G Uplink Channels,” *IEEE Wireless Communications Letters*, vol. 9, no. 6, pp. 851–855, 2020.
- [13] S. Lagen, K. Wanuga, H. Elkotby, S. Goyal, N. Patriciello, and L. Giupponi, “New radio physical layer abstraction for system-level simulations of 5g networks,” in *ICC 2020 - 2020 IEEE International Conference on Communications (ICC)*, 2020, pp. 1–7.
- [14] K. P. Srinath and J. Hoydis, “Bit-Metric Decoding Rate in Multi-User MIMO Systems: Applications,” 2022. [Online]. Available: <https://arxiv.org/abs/2203.06273>
- [15] M. Cirkic, D. Persson, and E. G. Larson, “Allocation of Computational Resources for Soft MIMO Detection,” *IEEE J. Sel. Topics in Signal Process.*, vol. 5, no. 8, pp. 1451–1461, 2011.
- [16] G. Caire, G. Taricco, and E. Biglieri, “Bit-Interleaved Coded Modulation,” *IEEE Trans. Inf. Theory*, vol. 44, no. 3, pp. 927–946, May 1998.
- [17] P. Fertl, J. Jalden, and G. Matz, “Capacity-based performance comparison of MIMO-BICM demodulators,” in *IEEE 9th Workshop on Signal Process. Advances in Wireless Commun.*, 2008, pp. 166–170.
- [18] K. Sayana, J. Zhuang, and K. Stewart, “Short term link performance modeling for ml receivers with mutual information per bit metrics,” in *IEEE GLOBECOM 2008 - 2008 IEEE Global Telecommunications Conference*, 2008, pp. 1–6.

- [19] 3GPP, “Evolved Universal Terrestrial Radio Access (E-UTRA); Physical channels and modulation,” 3rd Generation Partnership Project (3GPP), Technical Specification (TS) 36.211, 03 2020, version 16.4.0. [Online]. Available: <https://portal.3gpp.org/desktopmodules/Specifications/SpecificationDetails.aspx?specificationId=2425>
- [20] G. Böcherer, “Achievable Rates for Probabilistic Shaping,” 2018. [Online]. Available: <https://arxiv.org/abs/1707.01134>
- [21] S. Jaeckel, L. Raschkowski, K. Börner, and L. Thiele, “QuaDRiGa: A 3-D Multi-Cell Channel Model With Time Evolution for Enabling Virtual Field Trials,” *IEEE Trans. Antennas and Propag.*, vol. 62, no. 6, pp. 3242–3256, 2014.
- [22] S. M. Kay, *Fundamentals of Statistical Signal Processing: Estimation Theory*. USA: Prentice-Hall, Inc., 1993.
- [23] M. Goutay, F. Ait Aoudia, J. Hoydis, and J.-M. Gorce, “Machine Learning for MU-MIMO Receive Processing in OFDM Systems,” *IEEE Journal on Selected Areas in Communications*, vol. 39, no. 8, pp. 2318–2332, 2021.
- [24] C. McDiarmid, *Concentration*. Berlin, Heidelberg: Springer Berlin Heidelberg, 1998, pp. 195–248. [Online]. Available: https://doi.org/10.1007/978-3-662-12788-9_6
- [25] Y. LeCun, P. Haffner, L. Bottou, and Y. Bengio, *Object Recognition with Gradient-Based Learning*. Berlin, Heidelberg: Springer Berlin Heidelberg, 1999, pp. 319–345. [Online]. Available: https://doi.org/10.1007/3-540-46805-6_19
- [26] 3GPP, “Study on channel model for frequencies from 0.5 to 100 GHz,” 3rd Generation Partnership Project (3GPP), Technical Specification (TS) 38.901, 12 2019, version 16.1.0. [Online]. Available: <https://portal.3gpp.org/desktopmodules/Specifications/SpecificationDetails.aspx?specificationId=3173>
- [27] F. Ait Aoudia and J. Hoydis, “End-to-end learning for ofdm: From neural receivers to pilotless communication,” *IEEE Transactions on Wireless Communications*, vol. 21, no. 2, pp. 1049–1063, 2022.